

Supplement of Atmos. Chem. Phys., 14, 5183–5204, 2014
<http://www.atmos-chem-phys.net/acp-14-5183-2014/>
doi:10.5194/acp-14-5183-2014-supplement
© Author(s) 2014. CC Attribution 3.0 License.



Supplement of

H₂O and HCl trace gas kinetics on crystalline HCl hydrates and amorphous HCl/H₂O in the range 170 to 205 K: the HCl/H₂O phase diagram revisited

R. Iannarelli and M. J. Rossi

Correspondence to: M. J. Rossi (michel.rossi@psi.ch)

Supplement A

Detailed Description of Multidiagnostic Experiment.

The reactor consists of a high vacuum ($1 \cdot 10^{-7}$ Torr background pressure) stainless steel chamber in which controlled growth of thin ice films in the range 1-2 μm thickness is possible on a temperature-controlled Si substrate. It is equipped with the following diagnostic tools: Pfeiffer Vacuum QMS220 Quadrupole Mass Spectrometer (MS), BIORAD FTS-575C FTIR spectrometer equipped with a cryogenic HgCdTe detector and a MKS 627B Baratron absolute pressure gauge. The MS may be equipped with a Prisma™ or a PrismaPlus™ control unit depending on the measurement conditions, as will be explained below. The 1" diameter Si window, onto which gas condensation takes place, is the only cold surface in the reactor exposed to the admitted gases which allows the establishment of a 1:1 correspondence between changes in the gas and the thin film composition. Experimental proof beyond that given previously (Delval et al., 2003; Chiesa and Rossi, 2013) is given in the main text. The main difference to the reactor described by Delval et al. (2003) is the addition of a GENERAL VALVE CORPORATION Series 9 high speed solenoid valve of 2 mm orifice size controlled by an IOTA ONE driver unit for pulsed gas admission experiments (PV) as well as the introduction of an additional calibrated leak valve in a second bypass line to the MS chamber affording three different gas residence times in the stirred flow reactor (see Table 1 in main text). In PV experiments transient supersaturation of gas is obtained by injection of a short pulse of gas molecules of 5-20 milliseconds duration into the reactor. The additional bypass has a larger orifice and enables the extension of the pumping rate range from 0.171 to 0.811 s^{-1} for H_2O at 315 K.

The escape rate constant k_{esc} (s^{-1}) is proportional to the gas molar mass M ($\text{kg} \cdot \text{mol}^{-1}$) and the vessel temperature T (K) according to Eq. (S1):

$$k_{\text{esc}}(T, M) = \sqrt{\frac{8RT}{\pi M}} \cdot \frac{A_{\text{esc}}}{4V} = C \cdot \sqrt{\frac{T}{M}} \quad (\text{S1})$$

where R is the ideal gas constant in $\text{J} \cdot \text{mol}^{-1} \cdot \text{K}^{-1}$, A_{esc} the surface area of the effusion orifice in cm^2 , V the reactor volume in cm^3 and C the linear proportionality factor when M is expressed in $\text{g} \cdot \text{mol}^{-1}$. k_{esc} has been measured for the three possible combinations of two orifices (small open and large closed, small closed and large open, small and large open) using the effusion of non-reactive gases across both leak valves. For each inert gas used (H_2 , He, N_2 and Ar) a calibrated flow of molecules was established which was subsequently halted. The effusion of the gas from the reactor was monitored as a function of time using the MS and resulted in an exponential decay of the signal at the parent mass ($m/z = 2, 4, 28$ and 40 , respectively) whose decay rate was given by the effusion rate constant k_{esc} . The plot of the measured k_{esc} as a function of $\sqrt{\frac{T}{M}}$ provides the scaling factors C for the different orifice combinations, as reported in Table 1 in main text, and was used to scale k_{esc} for each gas (M) and temperature (T).

Three different operational conditions may be established: *static*, *dynamic* and *stirred flow*. Under *static* conditions the total pressure inside the reactor is monitored using the MKS Baratron absolute pressure gauge whereas the condensed phase is monitored by means of FTIR spectroscopy in transmission. *Dynamic* conditions are established by opening the 6" gate valve, thereby reaching the maximum pumping speed of $S = 190 \text{ l} \cdot \text{s}^{-1}$ in the reactor, corresponding to $k_{\text{esc}}^{\text{Dyn}} = 50 \cdot \text{s}^{-1}$ for H_2O . Under this condition, a typical flow of $F_i(\text{H}_2\text{O}) = 1 \cdot 10^{15} \text{ molec} \cdot \text{s}^{-1}$ of H_2O corresponds to a partial pressure of $2 \cdot 10^{-7}$ Torr in the reactor allowing

the use of MS to monitor the gas phase whereas the condensed phase is monitored by means of FTIR in transmission. *Stirred flow (SFR)* conditions are established when the gate valve is closed and either one or both calibrated leak valves are open. Under this condition, at a typical flow of $1 \cdot 10^{15}$ molec \cdot s $^{-1}$ of H₂O, the partial pressure in the reactor chamber varies between $9 \cdot 10^{-5}$ to $2 \cdot 10^{-5}$ Torr, when the small orifice is open or both leak valves are open, respectively. The gas phase is monitored by means of residual gas mass spectrometry in the lower chamber where the pressure remains lower than $2 \cdot 10^{-6}$ Torr at all operating conditions.

The temperature of the Si window is measured by means of a type T (copper/constantan) thermocouple wire clamped into a thermocouple well of the Si window support by a set screw and controlled by a PID program using LabVIEW™. The temperature accuracy in all experiments is ± 0.5 K. The temperature of the ice films grown on the Si window may be different from that of the window or support itself. The temperature is therefore calibrated using the vapour pressure of pure ice films measured under static conditions. A pure ice film of approximately 2 μ m thickness is grown by backfilling the reactor chamber with the introduction of a calibrated water vapour flow while the window is held at a temperature of approximately 180 K. The system is then set to static condition and the temperature slowly increased within the range 180 to 215 K. The equilibrium vapour pressure of water measured in the reactor as a function of temperature is then compared with literature results (Marti and Mauersberger, 1993). A correction of +2 to 3 K needs to be applied to the measured temperature in order to bring into agreement the equilibrium H₂O vapour pressure and the measured temperature of the Si window. The measured vapour pressure is also corrected to account for the difference in temperature between the ice surface (T_{ice}) and the reactor walls (T_w). Ideally, only T_{ice} of the condensed phase controls the equilibrium vapour pressure P_{eq} , but in practice we work with an experimental system whose walls are at temperature T_w that influences the measured partial pressure. In order to account for the phenomenon of thermal transpiration (Dushman and Lafferty, 1962), the measured vapour pressure P_{meas} has been corrected throughout this work, whenever it was necessary, according to equation S2:

$$P_{eq} = P_{meas} \sqrt{\frac{T_{ice}}{T_w}} \quad (S2)$$

The temperature of the reactor walls is set to a constant value $T_w = 315$ K, and thereafter we will refer to this temperature as “ambient” temperature.

In order to use the MS as a partial pressure or concentration monitor, a calibration of the MS signal for each gas of interest has been performed. When a gas X is injected into the reactor through the dosing tube at a flow rate $F_i(X)$, measured by means of a pressure drop in a calibrated volume, a mass spectrometric signal I_X is obtained. At steady state, the relation between the flow admitted and the MS signal obtained may be expressed by $F_i(X) = C_X \cdot I_X$ where $F_i(X)$ is the measured flow admitted in molec \cdot s $^{-1}$, I_X is the amplitude of the MS signal in A and C_X the calibration factor for the gas X in molec \cdot s $^{-1} \cdot$ A $^{-1}$. The calibration factor C_X may be measured under both dynamic and stirred flow conditions. For all gases used in this work, the calibration factors are identical for both SFR and dynamic conditions, as expected, within a typical experimental error of $\pm 5\%$, regardless of the measurement conditions. The calibration factors have been checked frequently throughout the study.

As mentioned above, FTIR spectroscopy in transmission has been used to monitor the condensed phase by collecting spectra averaging 8 scans at a resolution of 4 cm $^{-1}$ in the range 700-4000 cm $^{-1}$. Typical scan time is 45 to 60 seconds. FTIR spectroscopy has been used to measure the number of molecules deposited on the Si window if the molecular absorption cross-section is known. From the Beer-Lambert law, the relation for the absorption is as follows:

$$\text{OD} = \log\left(\frac{I_0}{I}\right) = 0.4343 \ln\left(\frac{I_0}{I}\right) \quad (\text{S3})$$

$$\ln\left(\frac{I_0}{I}\right) = \sigma \cdot n \cdot d \quad (\text{S4})$$

where OD is the optical density in absorbance units at a given wavelength and I_0 , I are the incident and transmitted intensities at the given wavelength, respectively, σ is the molecular absorption cross section in $\text{cm}^2 \cdot \text{molec}^{-1}$, n is the concentration in $\text{molec} \cdot \text{cm}^{-3}$ and d the optical pathlength in the absorber in cm. Equations S3 and S4 may be combined together to obtain the relation between OD and σ , namely $\ln(10) \cdot \text{OD} = \sigma \cdot n \cdot d$.

The volume of the optical sample is given by $V^{\text{FTIR}} = d \cdot A_{\text{Si}}$, where A_{Si} is the area of the film supported by the Si window ($A_{\text{Si}} = 0.99 \text{ cm}^2$, one side). Owing to the fact that the total number of molecules deposited on both sides of the Si support, namely N^{FTIR} , may be expressed as $N^{\text{FTIR}} = n \cdot V^{\text{FTIR}}$, it is then possible to calculate according to equation S5:

$$N^{\text{FTIR}} = \frac{\ln(10) \cdot \text{OD}}{\sigma} \cdot A_{\text{Si}} \quad (\text{S5})$$

The number of molecules in the solid phase has been used to establish the mass balance of the performed experiments (see main text).

In this study three different ice substrates have been used: pure ice films, crystalline $\text{HCl} \cdot 6\text{H}_2\text{O}$ films (HCl hexahydrate, thereafter HH) and amorphous HCl/ H_2O mixture films (thereafter amHCl).

The protocol for the growth of pure ice films is as follows: the chamber, under SFR conditions, is backfilled with bidistilled water vapour for a few minutes at flow rates between $5 \cdot 10^{15}$ - $10^{16} \text{ molec} \cdot \text{s}^{-1}$, with the Si substrate held at temperatures between 167-175 K. The film grows on both sides on the nominally 1" Si window to a thickness of typically 1 μm due to the backfilling procedure. The temperature of the support is then set to the desired value at a typical rate of $\pm 0.3 \text{ K min}^{-1}$.

The protocol for the growth of HH films is an extension of the one for pure ice films. After the growth of a pure ice film, the temperature of the Si substrate is held between 165-170 K and the sample is exposed to HCl vapour for roughly 10 minutes at flow rates between $7 \cdot 10^{14}$ - $1 \cdot 10^{15} \text{ molec} \cdot \text{s}^{-1}$ at typical vapour pressures P_{HCl} in the range 6 to $8 \cdot 10^{-6} \text{ Torr}$ at SFR conditions and under simultaneous monitoring of HCl at $m/z = 36$. A total dose of approximately $5 \cdot 10^{17}$ molecules of HCl is admitted into the reactor. It is important to notice that not all the admitted HCl molecules are adsorbed onto the ice film as roughly 50% of them are lost either through pumping across the effusion orifice or by adsorption onto the chamber walls. The mass balance for a few selected experiments will be displayed below. The formation of HH on the ice sample is monitored by means of FTIR absorption spectroscopy in transmission as a function of time, both during deposition of HCl and once the admission of HCl has been halted.

The protocol for the growth of amHCl films differs from the HH growth protocol only in the choice of temperature at which the sample is exposed to HCl. After the growth of the pure ice film, the temperature is increased to 175-178 K when a similar dose of HCl compared to HH growth is admitted into the reactor and monitored at $m/z = 36$ (HCl) and $m/z = 18$ (H_2O). Similarly, the formation of amHCl on the thin ice film sample is monitored using FTIR absorption spectroscopy.

Bibliography

Chiesa, S., and Rossi, M.J.: The Metastable $\text{HCl}\cdot 6\text{H}_2\text{O}$ phase – IR spectroscopy, phase transitions and kinetic/thermodynamic properties in the range 170-205 K, *Atmos. Chem. Phys. Discuss.* 13, 17793-17848, 2013. www.atmos-chem-phys-discuss.net/13/17793/2013/doi:10.5194/acpd-13-17793-2013.

Delval, C., Flückiger, B., and Rossi, M. J.: The rate of water vapor evaporation from ice substrates in the presence of HCl and HBr: implications for the lifetime of atmospheric ice particles, *Atmos. Chem. Phys.* 3, 1131–1145, 2003.

Marti J., and Mauersberger, K.: A Survey and New Measurements of Ice Vapor Pressure at Temperatures Between 170 and 250K, *Geophys. Res. Lett.* 20, 363-366, 1993.

Dushman, S., and Lafferty, J.M.: *Scientific Foundations of Vacuum Technique*, 2nd ed., John Wiley & Sons, New York, ch. 1, pg. 58, 1962.

Figures

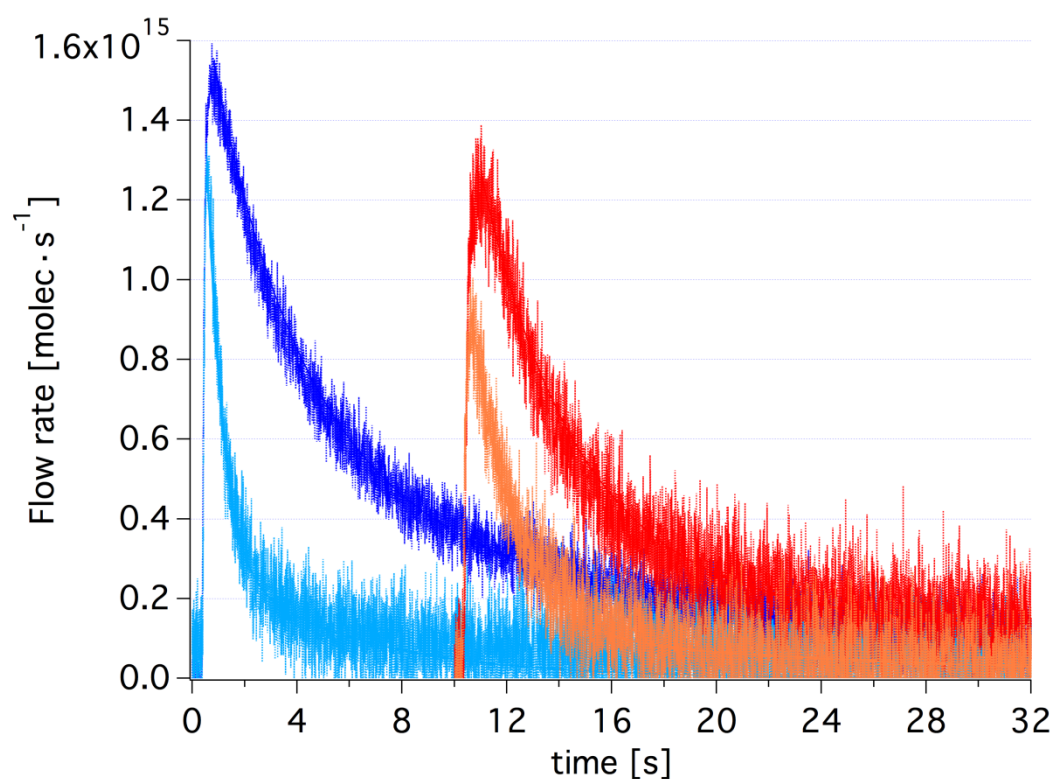


Figure S1: Pulses of HCl and H_2O . The dark blue curve is a pulse of $1.5\cdot 10^{16}$ molecule of H_2O ($m/z = 18$) admitted into the reactor with the cryostat at $T_w = 315$ K for the measurement of uptake on the reactor walls. Likewise, the red curve is a pulse of $4.7\cdot 10^{16}$ molecule of HCl ($m/z = 36$) admitted into the reactor at $T_w = 315$ K. The light blue curve is a pulse of $2.7\cdot 10^{16}$ molecule of H_2O admitted in the presence of an HH film at 185 K, the orange curve is a pulse of $3.4\cdot 10^{16}$ molecule of HCl admitted in the presence of an HH film at 170 K. An offset of 10 s has been applied to the HCl curves for clarity.

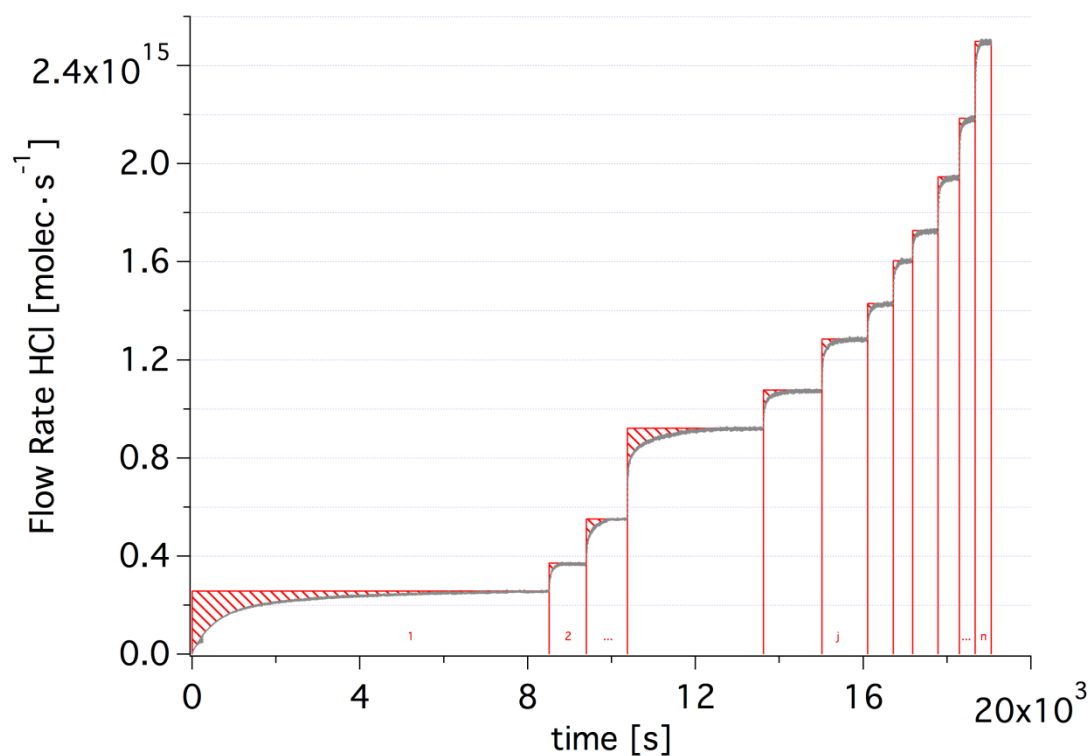


Figure S2: Calibrated MS signal for the adsorption of HCl onto the stainless-steel reactor walls. The red shaded area represents the cumulative loss of molecules to the reactor walls at each j -th time interval as a function of the flow rate or partial HCl pressure.

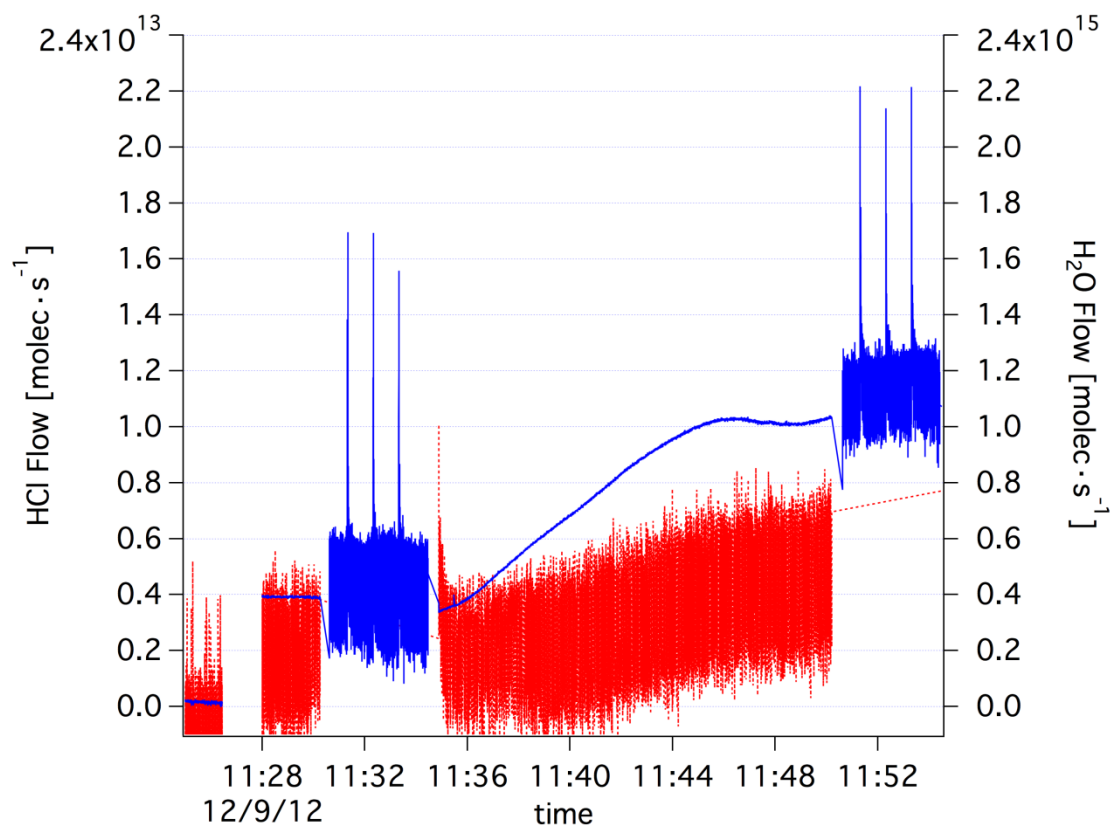


Figure S3: PV and steady state experiment at low temperatures as a function of time on HH substrates. The blue curve (right axis) represents the H_2O flow rate with a series of pulses at 176 and 181.5 K. The red curve (left axis) represents the corresponding HCl flow rate at the same temperatures. The flows of HCl and H_2O at

background are reported at the beginning of the time series for comparison. Similar results are obtained when pulses of HCl are admitted in the reactor. An example of HCl pulses in the presence of ice is displayed in orange in Fig. S1 compared to HCl pulses (red curve) in the absence of ice.

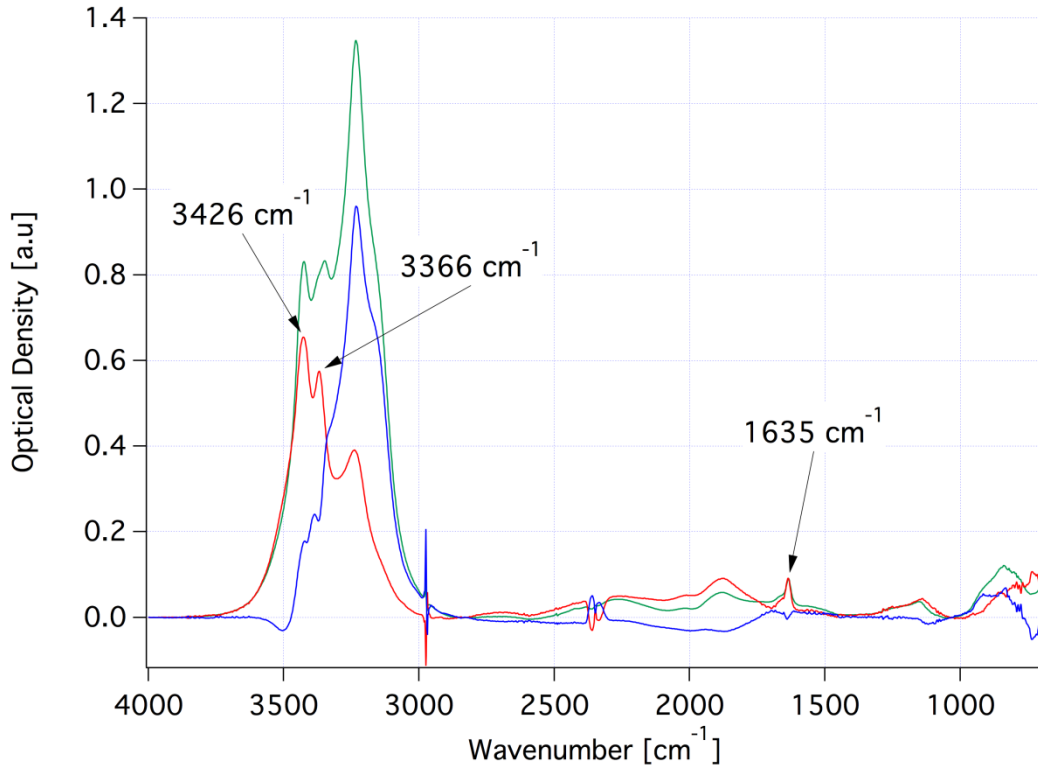


Figure A4: Deconvolution of a measured FTIR absorption spectrum of a H₂O/HH mixture using its pure ice (blue) and pure HH (red) components. The measured composite FTIR absorption spectrum is shown in green.

Supplement B

According to the scheme presented in reactions (R5-R10) in the main text, the following flow balance equation holds for a gas X (HCl, H₂O) in the stirred flow reactor (SFR):

$$F_{\text{in}}(\text{X}) + F_{\text{des}}(\text{X}) + F_{\text{ev}}(\text{X}) = F_{\text{SS}}(\text{X}) + F_{\text{ads,w}}(\text{X}) + F_{\text{ads,ice}}(\text{X}) \quad (\text{S6})$$

where all terms are flow rates in molec·s⁻¹. The interaction with the reactor walls is described by Langmuir type adsorption theory which assumes that a molecule can be adsorbed only on free specific surface sites.

The adsorption flux $J_{\text{ads,w}}$ in molec·s⁻¹·cm⁻² is given by Eq. (S7) (Crowley et al., 2010):

$$J_{\text{ads,w}}(\text{X}) = \frac{\alpha_w(\text{X}) \cdot \bar{c}}{4} (1 - \theta) \cdot [\text{X}] \quad (\text{S7})$$

where θ is the surface coverage, related to the surface concentration $[\text{X}]_s$ (in molec·cm⁻²) as $[\text{X}]_s = \theta \cdot N_{\text{MAX}}$ with N_{MAX} representing the maximum number of molecules that can be adsorbed per cm².

The thermally activated desorption flux from the walls J_{des} may be expressed as follows if a first order rate law for desorption is assumed:

$$J_{\text{des}}(\text{X}) = k_{\text{des}} \cdot [\text{X}]_s = k_{\text{des}} \cdot \theta \cdot N_{\text{MAX}} \quad (\text{S8})$$

Equilibrium is established when $J_{\text{ads,w}} = J_{\text{des}}$

$$\frac{\alpha_w(\mathbf{X}) \cdot \bar{c}}{4} (1-\theta) \cdot [\mathbf{X}] = k_{\text{des}} \cdot \theta \cdot N_{\text{MAX}} \quad (\text{S9})$$

which may be expressed in the form of a Langmuir isotherm as

$$\theta = \frac{K_L [\mathbf{X}]}{1 + K_L [\mathbf{X}]} \quad (\text{S10})$$

with the Langmuir constant of partition coefficient K_L ($\text{cm}^3 \cdot \text{molec}^{-1}$) given by:

$$K_L = \frac{\alpha_w(\mathbf{X}) \cdot \bar{c} / 4}{N_{\text{MAX}} \cdot k_{\text{des,w}}(\mathbf{X})} \quad (\text{S11})$$

The desorption rate constant $k_{\text{des,w}}$ is calculated from Eq. (S11) as:

$$k_{\text{des,w}}(\mathbf{X}) = \frac{\alpha_w(\mathbf{X}) \cdot \bar{c} / 4}{N_{\text{MAX}} \cdot K_L} \quad (\text{S12})$$

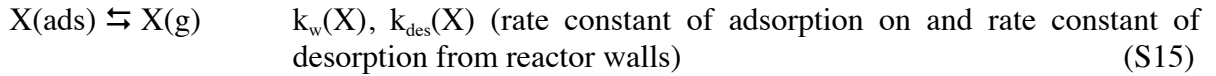
with K_L , N_{MAX} and α_w measured for the SRF according to the methods described in sections 3.1 and 3.2 in the main text. The flow balance Eq. (S6) may now be written as follow:

$$\begin{aligned} V \cdot R_{\text{in}}(\mathbf{X}) + S_w \cdot N_{\text{MAX}} \cdot k_{\text{des,w}}(\mathbf{X}) \cdot \theta + V \cdot R_{\text{ev}}(\mathbf{X}) &= \\ = V \cdot R_{\text{SS}}(\mathbf{X}) + S_w \cdot \frac{\alpha_w(\mathbf{X}) \cdot \bar{c}}{4} (1-\theta) \cdot [\mathbf{X}] + S_{\text{ice}} \cdot \frac{\alpha_{\text{ice}}(\mathbf{X}) \cdot \bar{c}}{4} \cdot [\mathbf{X}] & \end{aligned} \quad (\text{S13})$$

Substituting $S_w \cdot N_{\text{MAX}} = N_{\text{TOT}}$, the total number of molecules that can be adsorbed onto the total internal surface of the SFR, we may obtain Eq. (2) in the main text.

Supplement C

In order to describe the temporal evolution of the total number of molecules N in the SFR reactor in the aftermath of a pulse experiment, we will first describe the simpler case with no ice and extend it afterwards to the case in the presence of ice. In the absence of an ice film, the scheme presented in reactions (R5-R10) in the main text, can be simplified as follow for a gas X ($X = \text{HCl}, \text{H}_2\text{O}$):



In the aftermath of a pulse the following rate equation holds:

$$\frac{dN}{dt} = F_{\text{des}} - F_{\text{esc}} - F_{\text{ads}} \quad (\text{S16})$$

where all terms are flow rates in $\text{molec} \cdot \text{s}^{-1}$. N is the total number of molecules inside the reactor, F_{des} the desorption flow rate from the reactor walls, F_{esc} the effusion rate across the orifice and F_{ads} the adsorption flow rate onto the reactor walls, respectively. The number of molecules N may be expressed as $N = [\mathbf{X}] V$, where V is the total volume of the SFR. The flow rates may be given in terms of fluxes as $F_y = J_y \cdot S$, where S is the internal surface of the reactor and J_y is the corresponding flux. According to Eqs. (S6) and (S7), Eq. (S16) may be expressed as:

$$\frac{dN}{dt} = S \cdot k_{\text{des}} \cdot \theta \cdot N_{\text{MAX}} - k_{\text{esc}} \cdot N - S \cdot \frac{\alpha_w \cdot \bar{c}}{4} (1-\theta) \cdot \frac{N}{V} \quad (\text{S17})$$

In order to solve Eq. (S17) we assume that the desorption rate is low compared to adsorption processes so that at $t = 0$ there is no desorption from the walls. We may express the desorption term in Eq. (S17) as independent of N :

$$S \cdot k_{\text{des}} \cdot \theta \cdot N_{\text{MAX}} \cong k_{\text{des}} \cdot N_{\text{ADS}} \quad (\text{S18})$$

Furthermore, we assume that the coverage is small ($\theta \ll 1$) and therefore the adsorption term in Eq. (S17) may be expressed as:

$$S \cdot \frac{\alpha_w \cdot \bar{c}}{4} (1 - \theta) \cdot \frac{N}{V} \cong S \cdot \frac{\alpha_w \cdot \bar{c}}{4} \cdot \frac{N}{V} \quad (\text{S19})$$

Equation (S17) may then be rewritten as:

$$\frac{dN}{dt} = k_{\text{des}} \cdot N_{\text{ADS}} - N \cdot b, \quad b = \left(k_{\text{esc}} + \frac{S}{V} \cdot \frac{\alpha_w \cdot \bar{c}}{4} \right) \quad (\text{S20})$$

Equation (S20) is a linear differential equation that may be solved as sum of a homogeneous and an inhomogeneous part.

The solution for the homogeneous part is as follows:

$$\begin{aligned} \frac{dN}{dt} &= -N \cdot b \\ \int \frac{dN}{N} &= -\int b \cdot dt \\ N(t) &= C \cdot e^{-bt} \end{aligned} \quad (\text{S21})$$

For the inhomogeneous part the solution may be found as follows:

$$\begin{aligned} N(t) &= C(t) \cdot e^{-bt} \quad (\text{S22}) \\ \frac{dN}{dt} &= \frac{dC}{dt} \cdot e^{-bt} - b \cdot C(t) \cdot e^{-bt} \\ \frac{dN}{dt} &= \frac{dC}{dt} \cdot e^{-bt} - b \cdot N(t) \end{aligned} \quad (\text{S23})$$

From Eqs. (S20) and (S23) we may obtain:

$$k_{\text{des}} \cdot N_{\text{ADS}} - b \cdot N(t) = \frac{dC}{dt} \cdot e^{-bt} - b \cdot N(t)$$

from which follows:

$$\frac{dC}{dt} = k_{\text{des}} \cdot N_{\text{ADS}} \cdot e^{bt} \quad (\text{S24})$$

We assume an exponential decay for N_{ADS} :

$$N_{\text{ADS}} = N_{\text{ADS}}^0 \cdot e^{-k_{\text{des}} t} \quad (\text{S25})$$

Equation (S24) may be integrated as follows:

$$\int dC = k_{\text{des}} \cdot \int N_{\text{ADS}} \cdot e^{bt} \cdot dt \quad (\text{S26})$$

which gives after integration by parts:

$$k_{\text{des}} \cdot \int N_{\text{ADS}} \cdot e^{bt} \cdot dt = k_{\text{des}} \left(N_{\text{ADS}} \cdot \frac{e^{bt}}{b} - \int \frac{N_{\text{ADS}}}{dt} \cdot \frac{e^{bt}}{b} \cdot dt \right)$$

From Eq. (S25) we calculate the derivate of N_{ADS} and substitute, obtaining:

$$k_{\text{des}} \cdot \int N_{\text{ADS}} \cdot e^{bt} \cdot dt = k_{\text{des}} \left(N_{\text{ADS}} \cdot \frac{e^{bt}}{b} + \frac{k_{\text{des}}}{b} \cdot \int N_{\text{ADS}} \cdot e^{bt} \cdot dt \right)$$

$$\left(1 - \frac{k_{\text{des}}}{b} \right) \cdot k_{\text{des}} \cdot \int N_{\text{ADS}} \cdot e^{bt} \cdot dt = k_{\text{des}} \cdot N_{\text{ADS}} \cdot \frac{e^{bt}}{b}$$

$$k_{\text{des}} \cdot \int N_{\text{ADS}} \cdot e^{bt} \cdot dt = \frac{k_{\text{des}}/b \cdot N_{\text{ADS}} \cdot e^{bt}}{\left(1 - k_{\text{des}}/b \right)} \quad (\text{S27})$$

From Eqs. (S26) and (S27) we may obtain:

$$C(t) = \frac{k_{\text{des}}/b \cdot N_{\text{ADS}} \cdot e^{bt}}{\left(1 - k_{\text{des}}/b \right)} + C_0 \quad (\text{S28})$$

And therefore obtain $N(t)$ in Eq. (S22):

$$N(t) = \frac{k_{\text{des}}/b \cdot N_{\text{ADS}}}{\left(1 - k_{\text{des}}/b \right)} + C_0 \cdot e^{-bt} \quad (\text{S29})$$

At $t = 0$ we have $N(t) = N_0$, the number of molecules introduced in a pulse

$$C_0 = N_0 - \frac{k_{\text{des}}/b \cdot N_{\text{ADS}}}{\left(1 - k_{\text{des}}/b \right)}$$

from which follows, together with Eq. (S25):

$$N(t) = N_0 \cdot e^{-bt} + \frac{k_{\text{des}}/b \cdot N_{\text{ADS}}^0 \cdot e^{-k_{\text{des}}t}}{\left(1 - k_{\text{des}}/b \right)} \left(1 - e^{-bt} \right) \quad (\text{S30})$$

The solution presented in Eq. (S30) can be extended under the same assumptions to the case where ice is present by introducing a term similar to b that contains all loss processes:

$$d = \left(k_{\text{esc}} + \frac{S}{V} \cdot \frac{\alpha_w \cdot \bar{c}}{4} + \frac{S_{\text{ice}}}{V} \cdot \frac{\alpha_{\text{ice}} \cdot \bar{c}}{4} \right)$$

The governing equation in the presence of ice is:

$$\frac{dN}{dt} = k_{\text{des}} \cdot N_{\text{ADS}} + k_{\text{ev}} \cdot N_{\text{ev}} - N \cdot d \quad (\text{S31})$$

where k_{ev} and N_{ev} are the rate constant of evaporation from the ice and the number of molecules adsorbed on the ice sample and evaporating from it, respectively.

With a mathematical derivation similar to the case in the absence of ice a solution for $N(t)$ can be derived as reported in Eq. (S32):

$$N(t) = N_0 \cdot e^{-dt} + (1 - e^{-dt}) \left(\frac{k_{\text{des}}/d \cdot N_{\text{ADS}}^0 \cdot e^{-k_{\text{des}}t}}{(1 - k_{\text{des}}/d)} + \frac{k_{\text{ev}}/d \cdot N_{\text{ev}}^0 \cdot e^{-k_{\text{ev}}t}}{(1 - k_{\text{ev}}/d)} \right) \quad (\text{S32})$$

Equation (S32) represents the general solution for the fitting procedure of pulse experiments as a superposition of a fast decay given by the sum of all loss processes, $N_0 \cdot e^{-dt}$, and a slower term which accounts for slower processes of evaporation from the ice and desorption from the walls.

Supplement D

Pulse fitting procedure

Figure S5 shows an example of the fitting procedure used to measure k_{ice} of HCl interacting with ice in the aftermath of a PV experiment. The grey line is the calibrated MS signal at m/z 36. Under the assumption that the desorption is slow compared to the fast adsorption processes it is possible to describe the decay of the signal as a sum of exponentials. A fast decay given by $k_d = k_{\text{esc}} + k_w + k_{\text{ice}}$ in the first 3 to 4 seconds after the pulse is superimposed on a slow desorption which becomes important once fast adsorption has subsided. The red curve shows a fit of a fast exponential decay associated to k_d . It is obvious that a simple adsorption process cannot accurately describe the behaviour of the measured signal, especially at longer decay times in the tail of the decay trace. The black curve shows a fit given by a superposition of a fast exponential decay k_d and a slower processes of evaporation from the ice and desorption from the walls. Good agreement is found with the measured calibrated signal of HCl.

All pulses measured during this work have been treated using the same assumptions and the best fit has been obtained for all decays in order to determine k_d and α_{ice} according to Eq. (10) in the main text. Supplement C reports the mathematical derivation of the analytical form of the best fit of a pulse decay in the absence and in the presence of an ice sample.

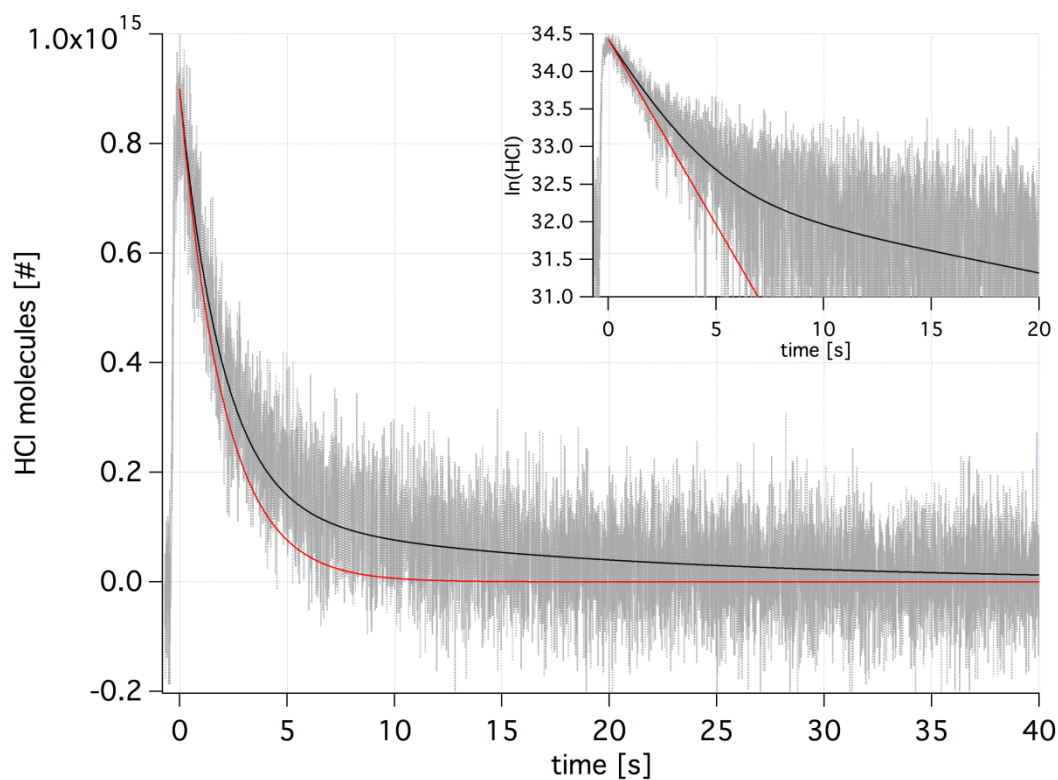


Figure S5: Real time HCl PV experiment in the presence of ice at $T = 189.5$ K. The measured HCl calibrated signal is shown in grey as a function of time. In red and black fit curves of the signal. The red curve is calculated fitting the curve with an exponential decay whose constant is given by $k_d = k_{esc} + k_w + k_{ice}$. The black fit is calculated considering the signal decay as sum of a fast decay k_d and a slow desorption contribution from the walls and the ice. The insert shows the signal and the fits on a semi-logarithmic scale.

Bibliography

Crowley, J.N., Ammann, M., Cox, R.A., Hynes, R.G., Jenkin, M.E., Mellouki, A., Rossi, M.J., Troe, J., and Wallington, T.J.: Evaluated kinetic and photochemical data for atmospheric chemistry: Volume V – heterogeneous reactions on solid substrates, *Atmos. Chem. Phys.* 10, 9059-9223, 2010.